Supplementary information

Simultaneous ambient long-term conductivity promotion, interfacial modification, ion migration inhibition and anti-deliquescence by MWCNT:NiO in spiro-OMeTAD for perovskite solar cells

Yanjing Rong,[a] Mengqi Jin,[a] Qing Du,[a] Zhitao Shen,[a] Yan Feng, [a] Mengxin Wang,[a] Fumin Li,[a] Rong Liu, [a] Huilin Li, [a] Chong Chen[a]*

[a] Henan Key Laboratory of Photovoltaic Materials, Henan University, Kaifeng 475004, P. R. China

1. First-principles calculations

Electronic structure calculations were performed with the density functional theory as implemented in the Vienna ab initio simulation package,[1-2] employing the projected augmented wave potentials[3] to describe the atomic core electrons and the plane wave basis set to expand the Kohn−Sham electronic states. For the exchange and correlation functional, the generalized gradient approximation (GGA) in the Perdew–Burke–Ernzerhof (PBE) format was used.[4] The kinetic energy cutoff was set to 400 eV for all calculations in this work.

The bulk structure of NiO was first optimized based on the XRD experimental data. According to experiment,[5] NiO has a cubic phase with a space group of Fm-3m, and $a = b = c = 4.18000$ Å. The computational cell parameters are $a = b = c = 4.14250$ Å in this work, which agrees well with the experimental data. In the bulk structure relaxation, the Brillouin zone was sampled by a (6 × 6 ×6) k-points mesh with Gamma point centered. All the atoms and cell parameters were fully relaxed until the atomic forces are less than 0.01 eV Å^{-1}.

In order to account for interactions between Li-TFSI ($C_2F_6LiNO_4S_2$) and NiO, the (110) surface of NiO with dimensions of 4.14250 Å × 11.7168 Å and with a thickness of 3.5 Å was constructed, and then it was combined with Li-TFSI. A vacuum thickness of 30 Å was added along the z direction to avoid spurious interaction between slab images. The Brillouin zone was sampled by 5 × 2 × 1 gamma centered k-point meshes. During structural optimization, all the atoms were fully relaxed until the atomic forces are less than 0.05 eV Å^{-1}.

In order to account for interactions between $CsPbI_3$ and NiO, a periodic slab model was constructed. A 2 × 1 (12.7226 × 6.3613 Å) $CsPbI_3$ (001) surface supercell with 6 atomic layers was cut from the crystal structure. Similarly, a 2 × 1 (12.4275 × 4.14250Å) NiO (001) surface supercell with 3 atomic layers was cut from the computed crystal structure. And then the $CsPbI_3$ (001) surface was contacted with the NiO (001) surface. In the

E-mail: chongchen@henu.edu.cn (C. Chen).

z direction, a 30 Å vacuum layer was added to avoid interaction between slab and its image. The Brillouin zones was sampled by 2 × 5 × 1 gamma centered k-point meshes. All the atoms and cell parameters were full relaxed until the residual force was less than 0.02 eV $Å^{-1}$.

In addition, to consider the van der Waals interactions, the DFT-D3 method with Becke-Jonson damping[6] was used for all the calculations. The visualizations of the crystal structure and the charge density were by virtue of the VESTA code.[7]

References:

[1] G. Kresse, J. Furthmuller, *Phys Rev B.* **1996**, 54, 11169.

[2] G. Kresse, J. Hafner, *Phys Rev B.* **1993**, 47, R558.

[3] P. E. Blochl, *Phys Rev B.* **1994**, 50, 17953.

[4] J. P. Perdew, K. Burke, M. Ernzerhof, *Phys Rev Lett.* **1996**, 77, 3865.

[5] I. M. Steele1, J. J. Pluth, *J. Am. Chem. Soc.* **1936**, 58, 173.

[6] S. Grimme, S. Ehrlich, L. Goerigk, *J. Comp. Chem.* **2011**, 32, 1456.

[7] K. Momma, F. Izumi, *J. Appl. Crystallogr.* **2011**, 44, 1272.

2. Figures and Figure Captions for Supporting Information

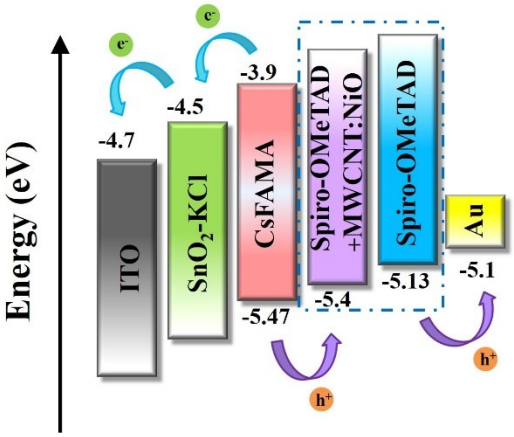

Figure S1. Energy level diagrams of PSCs.

Tabe S1. The conductivity σ (S cm^{-1}) of the three different types of devices.

Devices	0 days	8 days	18 days	30 days	43 days
spiro-OMeTAD	7.60	9.21	8.17	6.50	5.52
spiro-OMeTAD+ MWCNT	9.08	10.84	9.82	8.57	7.69
spiro-OMeTAD+ MWCNT: NiO	11.55	12.86	12.58	11.31	10.61

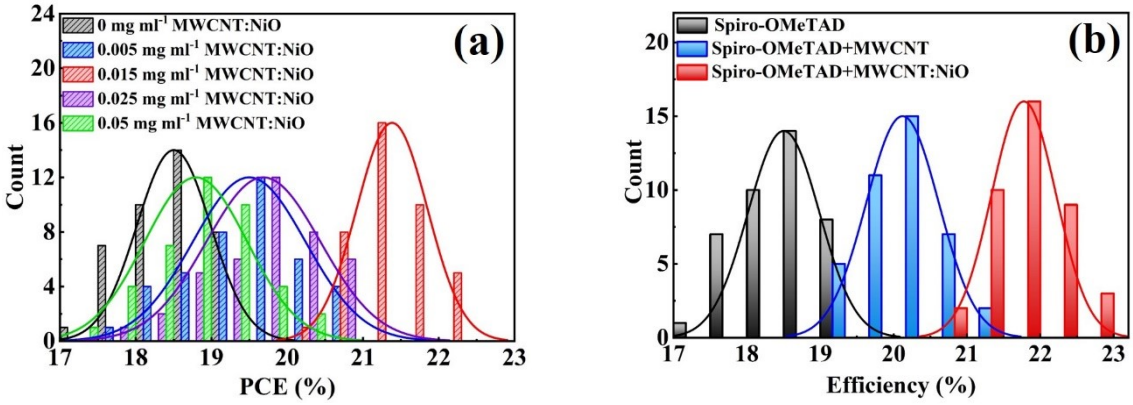

Figure S2. (a) PCE histograms of the 40 PSCs devices based on MWCNT:NiO with different concentrations. (b) The histograms of PCE values obtained from 40 PSCs of each set.

Table S2. Device performance parameters of 40 PSCs with different concentrations of MWCNT:NiO.

MWCNT:NiO concentration	V_{oc} (V)	J_{sc} (mA cm^{-2})	FF	PCE (%)	Average PCE (%)
0 mg ml^{-1}	1.15 ± 0.02	22.88 ± 0.25	0.73 ± 0.01	19.21	18.50 ± 0.71
0.005 mg ml^{-1}	1.15 ± 0.02	24.28 ± 0.18	0.74 ± 0.02	20.67	19.95 ± 0.72
0.015 mg ml^{-1}	1.17 ± 0.02	24.91 ± 0.14	0.77 ± 0.01	22.73	22.02 ± 0.71
0.025 mg ml^{-1}	1.15 ± 0.02	24.54 ± 0.23	0.75 ± 0.01	21.17	20.43 ± 0.74
0.05 mg ml^{-1}	1.14 ± 0.03	24.08 ± 0.28	0.74 ± 0.02	20.31	19.58 ± 0.73

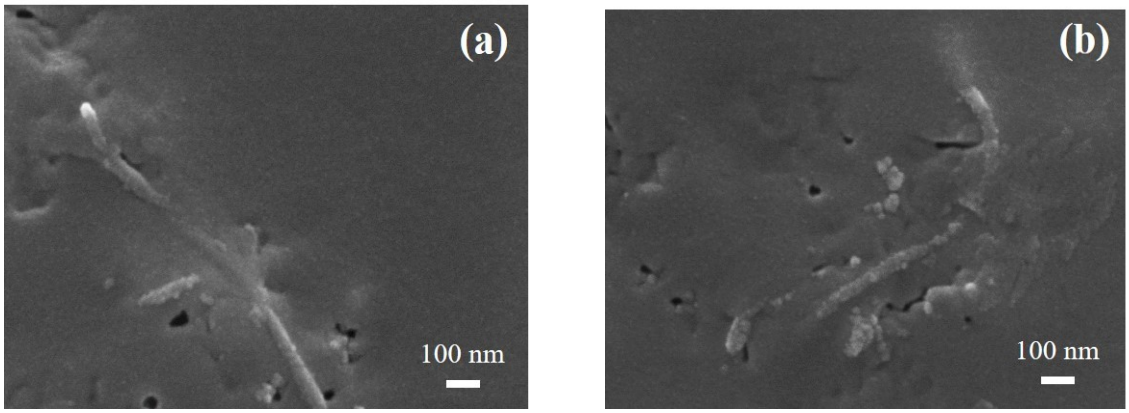

Figure S3. (a) Top-view SEM images of spiro-OMeTAD with MWCNT layer (0.1mg ml^{-1}) and (b) spiro-OMeTAD with MWCNT:NiO layer (0.1mg ml^{-1}) coated on a glass substrate.

Tabe S3. Device performance parameters of 40 PSCs with different concentrations of MWCNT.

MWCNT concentration	V_{oc} (V)	J_{sc} (mA cm^{-2})	FF	PCE (%)	Average PCE (%)
0 mg ml^{-1}	1.15 ± 0.02	22.88 ± 0.25	0.73 ± 0.01	19.21	18.50 ± 0.71
0.005 mg ml^{-1}	1.15 ± 0.02	23.77 ± 0.13	0.74 ± 0.01	20.23	19.48 ± 0.75
0.015 mg ml^{-1}	1.16 ± 0.02	24.29 ± 0.15	0.75 ± 0.01	21.13	20.42 ± 0.71
0.025 mg ml^{-1}	1.15 ± 0.02	24.10 ± 0.12	0.75 ± 0.01	20.79	20.06 ± 0.73
0.05 mg ml^{-1}	1.14 ± 0.03	23.66 ± 0.98	0.74 ± 0.02	19.96	19.22 ± 0.74

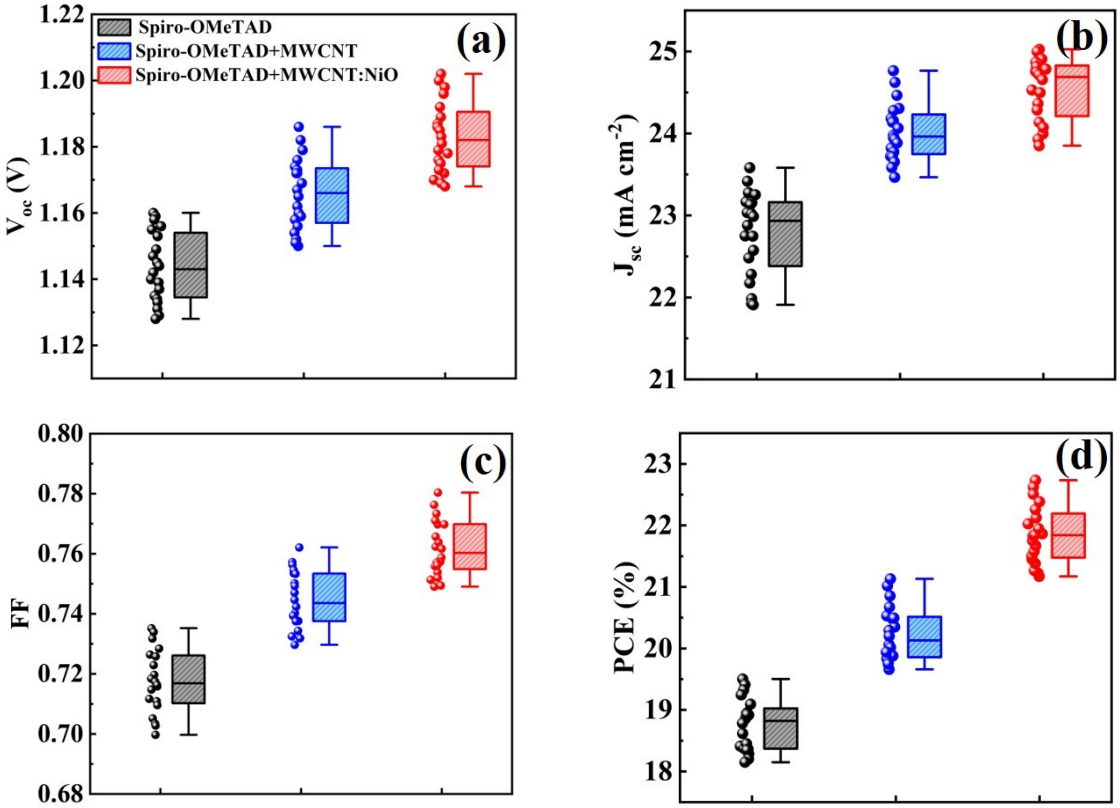

Figure S4. The parameters statistical diagrams of 20 PSCs devices with spiro-OMeTAD, sprio-OMeTAD+MWCNT and sprio-OMeTAD+MWCNT:NiO. (a) V_{oc}, (b) J_{sc}, (c) FF, (d) PCE.

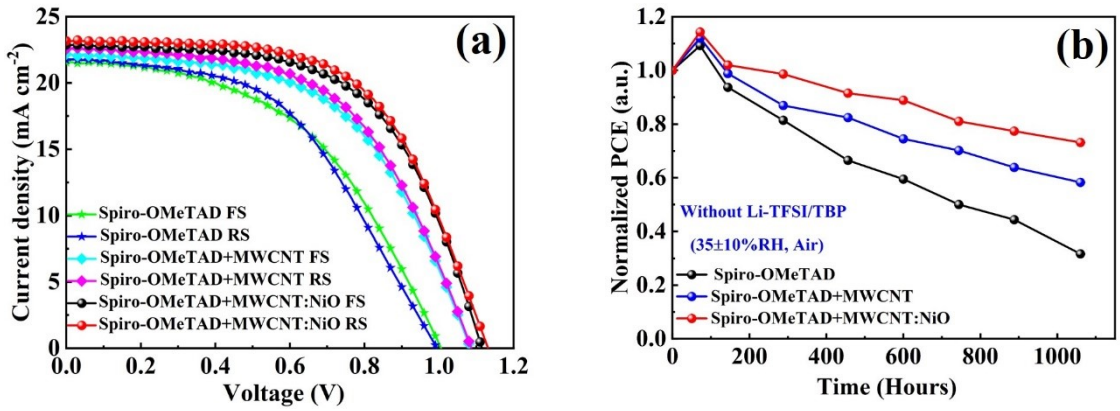

Figure S5. (a) *J-V* curves of the best devices of PSCs based on different HTLs (without Li-TFSI/tBP). (b) Long-term stability measurements.

Tabe S4. Performance parameters of three different types of devices without Li-TFSI under AM 1.5G 1 sun illumination.

Devices	V_{oc} (V)	J_{sc} (mA cm^{-2})	FF	PCE (%)
spiro-OMeTAD FS	0.94	21.86	0.44	9.15
spiro-OMeTAD RS	0.95	22.05	0.45	9.24
spiro-OMeTAD+ MWCNT FS	1.08	22.39	0.52	12.51
spiro-OMeTAD+ MWCNT RS	1.09	22.56	0.56	13.64
spiro-OMeTAD+ MWCNT: NiO FS	1.12	22.92	0.57	14.75
spiro-OMeTAD+ MWCNT: NiO RS	1.13	23.17	0.59	15.53

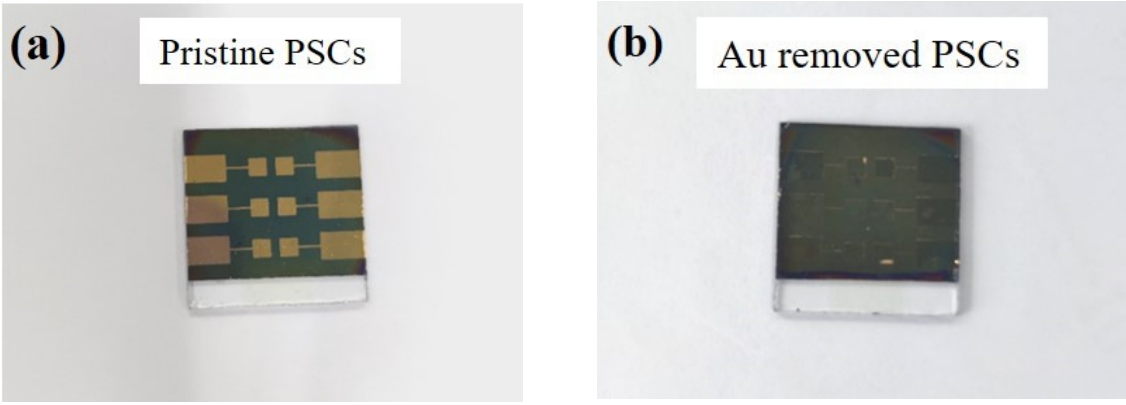

Figure S6. Photographs of PSCs before (a) and after (b) removing Au electrode with tape. The specific electrode removing process is shown in movie S1.

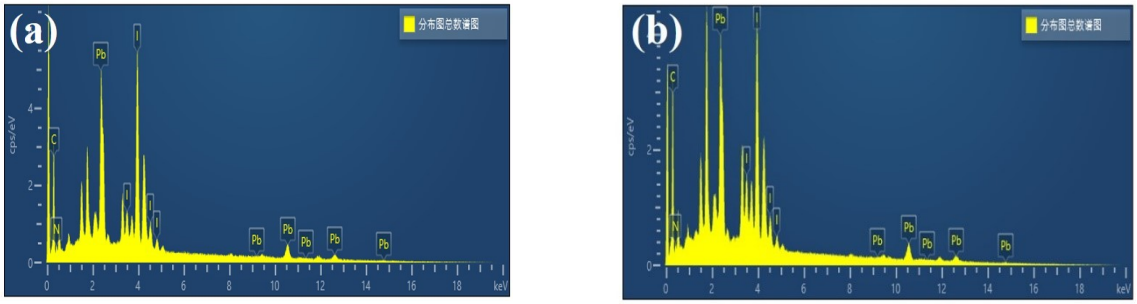

Figure S7. Total element spectra during SEM-EDX mapping of (a) spiro-OMeTAD and (b) spiro-OMeTAD+MWCNT:NiO film.

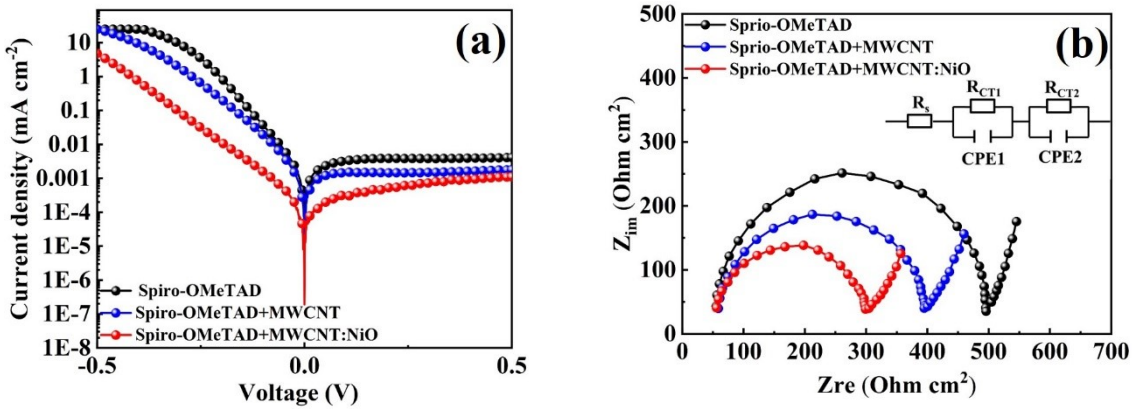

Figure S8. (a) *J-V* characteristics of PSCs swept from -0.5 V to 0.5 V in the dark. (b) Electrochemical impedance spectra (EIS) for the control, MWCNT-doped PSCs and MWCNT:NiO-doped PSCs under illumination100 mW cm^{-2}.

Tabe S5. The fitting parameters for measured EIS results with three different types of devices.

Devices	R_s (Ω cm^{-2})	R_{CT1} (Ω cm^{-2})	R_{CT2} (Ω cm^{-2})	CPE1 (μF cm^{-2})	CPE2 (nF cm^{-2})
spiro-OMeTAD	56.22	3282	432.6	3.06	1.08
spiro-OMeTAD+MWCNT	55.18	3041	329.9	3.09	1.35
spiro-OMeTAD+MWCNT:NiO	51.44	2462	243.7	2.40	2.06

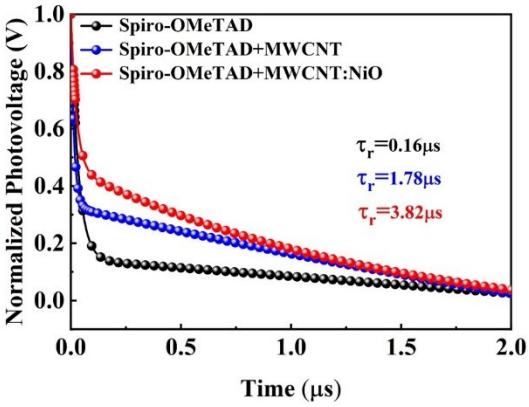

Figure S9. Transient photovoltage (TPV) decay.

Tabe S6. Parameters of bi-exponential fitting for TPV decay traces of three different types of devices.

Device	A_1	τ_1(s)	A_2	τ_2(s)	τ_r(μs)
spiro-OMeTAD	0.554	3.39E-8	0.141	6.94E-7	0.16
spiro-OMeTAD+MWCNT	0.194	2.57E-8	0.366	2.68E-6	1.78
spiro-OMeTAD+MWCNT:NiO	0.259	1.43E-8	0.422	6.17E-6	3.82